American Mineralogist, Volume 62, pages 229–245, 1977

Samuelsonite: its crystal structure and relation to apatite and octacalcium phosphate

PAUL B. MOORE AND TAKAHARU ARAKI

Department of the Geophysical Sciences
The University of Chicago
Chicago, Illinois 60637

Abstract

Samuelsonite, $(Ba_{0.42}\square_{0.58})(Ca_{0.46}\square_{0.54})_2(Mn^{2+}_{0.45}Fe^{2+}_{0.30}Na^{1+}_{0.25})_4Ca_8Al_2(OH)_2(PO_4)_{10}$, monoclinic, a 18.495(10), b 6.805(4), c 14.000(8) Å, β 112.75(6)°, space group $C2/m$, $Z = 2$, is a novel structure type related to apatite and octacalcium phosphate. $R = 0.084$ for 2571 independent reflections.

Samuelsonite, apatite, and octacalcium phosphate contain regions in their structures which are isomorphic to each other. Beyond these regions, structural isomorphism ceases to exist. The underlying unit is a column of composition $[Ca_4(PO_4)_{12}]$. In samuelsonite, this unit is fused by a screw axis to form double columns of composition $[Ca_4(PO_4)_{10}]$; in octacalcium phosphate, sheets are generated by inversion centers to form $[Ca_4(PO_4)_8]$; in apatite, the columns form a framework of composition $[Ca_4(PO_4)_6]$. A related column occurs in the crystal structure of hanksite, $Na_{20}(CO_3)_2Cl[KNa_2(SO_4)_9]$.

Hypotheses are advanced for growth of apatite, whose central argument is the inherent stability of the $[Ca_4(PO_4)_{12}]$ columns; disorder and calcium deficiencies in some apatites may arise from the rotational disorder of the cylindrical dense-packing of the columns.

Introduction

Samuelsonite, $(Ca,Ba)Fe^{2+}_2Mn^{2+}_2Ca_8Al_2(OH)_2(PO_4)_{10}$, is a new mineral from the famous Palermo No. 1 pegmatite, North Groton, New Hampshire. Moore *et al.* (1975) noted that the species occurs in two distinct paragenetic settings, the one as small lustrous prismatic crystals in cavities of whitlockite–carbonate apatite–siderite rock, the other as large (up to 4 cm) bladed aggregates in association with a disintegrated phosphate pod (heterosite?). A structural kinship to apatite was recognized which, in relationship with octacalcium phosphate, $Ca_8H_2(PO_4)_6 \cdot 5H_2O$, adds interest to the species. In addition, the complex crystal chemistry of samuelsonite did not admit certain interpretation of its composition in absence of knowledge of its atomic positions and their populations, and structure analysis was necessary to resolve these arguments.

Samuelsonite possesses a noteworthy structure, allied to apatite and octacalcium phosphate. With its structure at hand, we conclude this paper with some speculations on apatite stability and advance an hypothesis to rationalize fragmented units of the apatite structure which are now known to persist in other structure types.

Experimental section

A single crystal of samuelsonite was selected from the type material and prepared for a three-dimensional data set from a *Pailred* automated diffractometer. We adopted the crystal cell data from Moore *et al.* (1975) and summarize these results in Table 1.

Table 1 also outlines the experimental details of the structure study. Owing to the thin and elongate habit of the crystal, eight facets were selected to approximate a polyhedral shape suitable for absorption correction on the basis of a Gaussian integration method (Burnham, 1966). Estimated errors of the intensities (σ_I) were calculated from $\sigma_I^2 = S + t^2B$ where S = peak scan counts, B = total background counts, and t = ratio of peak to background times. For the reflections with $I < 2\sigma_I$, we set $I = \sigma_I$. The σ_I's were then converted directly to the estimated errors in structure factors.

There were 2571 independent F_o available for study, but we photographically estimated 19 additional reflections within the blind region of the diffractometer and used these only for the Patterson synthesis. The space group $C2/m$ was checked for centrosymmetry by the $N(z)$ (Howells *et al.*, 1950) test on special projections and the $P(y)$ (Srikrishnan

TABLE 1. Samuelsonite. Experimental section

(A) Crystal Cell Data

a(Å)	18.495(10)
b(Å)	6.805(4)
c(Å)	14.000(8)
β (degrees)	112.75(6)
Space group	C2/m
Z	2
Formula*	$(Ba_{0.42},\square_{0.58})(Ca_{0.46},\square_{0.54})_2(Mn^{2+}_{0.45},Fe^{2+}_{0.30},Na^{1+}_{0.25})_4$ $Ca_8Al_2(OH)_2(PO_4)_{10}$
ρ(calc, gm cm^{-3})	3.355
Specific gravity	3.353
μ(cm^{-1})	38.4

(B) Intensity Measurements

Crystal size (mm)	0.024 (||[$\bar{1}$01]), 0.150 (\|\|[10$\bar{1}$]), 0.760 (||[010])
Crystal orientation	ϕ-axis = [010]
Maximum sinθ/λ	0.70
Scan speed	1.0° min^{-1}
Base scan width	3.8° (to 7.8° for manually scanned strong reflections)
Background counts	Stationary, 20 sec at beginning and end of scan
Radiation	MoKα_1 (λ = 0.70926Å), graphite monochromator
Independent F_o	2571

(C) Refinement of the Structure

R	0.084
R_w	0.108
Scale factor	1.440(8)
Goodness of fit†	5.03

*From refined crystal structure.

†Defined as $\Sigma_w||F_o|-|F_c||^2/(n-m)$ where n = number of independent F's and m = number of parameters.

and Parthasarathy, 1970) test on general reflections. These tests showed intensity distribution indicating a centrosymmetric crystal. Throughout the study, there was no reason to question the space group $C2/m$, and the success of the structure analysis is adopted as the test for its correctness.

Analysis of the structure

A three-dimensional Patterson synthesis, $P(uvw)$, revealed that most atoms were situated at $y = 0$ and $\frac{1}{2}$ with some additional contributions at $y \sim \pm \frac{1}{4}$. The mirror planes place severe restrictions on atom locations since $b/2 = 3.40$ Å. Several models satisfied the stronger vector densities of $P(uvw)$, and we suspected a strong homometric character of the analysis. Despite this impediment, a satisfactory solution was found, attested by spherical contours on the trial β-synthesis (see Ramachandran and Srinivasan, 1970). At this stage, it was possible to identify five independent $[PO_4]$ tetrahedra, an Al–O octahedron and five independent metal positions. Least-squares refinement followed by a γ'-synthesis revealed two additional weak electron density distributions at ½ ½ ½ and 0.418, 0, 0.413.

Moore *et al.* (1975) obtained the cell contents (based on $\Sigma O = 84$) $Ba_{1.00}Sr_{0.09}Na_{1.47}Ca_{17.20}Mn_{3.63}Fe_{2.94}Al_{3.96}H_{4.03}P_{20.18}O_{84.00}$. Trial bond distance calculations suggested that the occupancy at ½ ½ ½ [called $X(1)$] included a large cation, specifically Ba^{2+}; and that the occupancy at 0.418, 0, 0.413 [called $X(2)$] was

probably partly occupied Ca^{2+}. In addition, $X(1)$ or $X(2)$ can be at most only half-filled if both accommodate cations, since the distance $X(1)$–$X(2)$ = 1.53 Å. Appealing to the above composition of the crystal (Table 1) we set $X(1) = Ba^{2+}$ and $X(2) = Ca^{2+}$. Two metal positions, $M(1)$ and $M(2)$, define octahedral edge-sharing chains, and their distances suggested that the octahedra were occupied by the transition metals. The remaining three positions, Ca(1), Ca(2), and Ca(3), afforded distances typical for Ca–O.

In the next stage of the structure analysis we proposed to vary the occupancies for $X(1)$ applying the scattering curve for Ba^{2+} and for $X(2)$ with the curve for Ca^{2+}. The electron density distributions for $M(1)$ and $M(2)$ were low for Fe^{2+} and Mn^{2+}, and we assumed that Na^{1+} substituted at these sites. Since there were no steric reasons for partial occupancies at the centers of the octahedral chains, we concluded the sites were fully occupied by mixed transition metals and Na^{1+}. For $M(1)$ and $M(2)$, we applied scattering curves for Fe^{2+} and Na^{1+}, varying their contribution according to Finger (1968). The curve for Ca^{2+} was applied to Ca(1), Ca(2), and Ca(3); Al^{3+} for Al; P^{2+} for P; and O^{1-} for O utilizing the scattering factors of Cromer and Mann (1968).

At the final stage of refinement, one scale factor, one extinction coefficient (Zachariasen, 1968), 2 site occupancies, 2 scattering curve parameters, 59 atomic coordinate parameters, and 130 anisotropic thermal vibration parameters were varied. This corresponds to a data-to-variable parameter ratio of about 13:1. The refinement converged to the results in Table 1 where

$$R = \frac{\Sigma||F_o| - |F_c||}{\Sigma|F_o|}$$

$$R_w = \left[\frac{\Sigma w(|F_o| - |F_c|)^2}{\Sigma w|F_o|^2}\right]^{1/2}$$

with $w = \sigma^{-2}$ of F_o.

The atomic coordinate parameters appear in Table 2; Table 3 presents the anisotropic thermal vibration parameters, Table 4 the root mean square displacements and their crystallographic orientations, and Table 5 the structure factors.[1]

Discussion on the site population assignments is now in order. The Ca(1), Ca(2), and Ca(3) positions are essentially occupied by Ca^{2+}, and these sites are

[1] To obtain a copy of this table, order Document AM-76-037 from the Business Office, Mineralogical Society of America, 1909 K Street, N.W., Washington, D. C., 20006. Please remit $1.00 in advance for the microfiche.

TABLE 2. Samuelsonite. Atomic coordinate parameters*

Atom†	x	y	z	Atom	x	y	z
X(1)	1/2	1/2	1/2	P(3)	.1868(1)	0	.4461(2)
X(2)	0.4184(3)	1/2	0.4133(3)	O(7)	.2642(4)	0	.4304(5)
				O(8)	.2037(4)	0	.5601(5)
M(1)	0	0.2376(2)	0	O(9)	.1403(3)	.1803(6)	.3901(3)
M(2)	.0607(1)	.0000	.2466(1)				
				P(4)	.0772(1)	1/2	.1579(2)
Ca(1)	.4103(1)	0	.1575(1)	O(10)	.0834(4)	1/2	.0516(5)
Ca(2)	.1163(1)	1/2	.4246(1)	O(11)	.1545(4)	1/2	.2492(5)
Ca(3)	.2584(1)	.2528(2)	.3058(1)	O(12)	.0278(3)	.3172(6)	.1594(3)
P(1)	.1622(1)	0	.1046(2)				
O(1)	.0751(4)	0	.0284(5)	P(5)	.3665(1)	1/2	.1831(2)
O(2)	.1634(4)	0	.2156(5)	O(13)	.3192(4)	1/2	.2509(5)
O(3)	.2054(2)	.1838(6)	.0947(3)	O(14)	.4539(4)	1/2	.2540(5)
				O(15)	.3467(3)	.3147(6)	.1131(3)
P(2)	.4126(1)	0	.3714(2)				
O(4)	.3386(4)	0	.2716(5)	OH	.2081(3)	1/2	-.0031(5)
O(5)	.4816(4)	0	.3388(5)				
O(6)	.4087(3)	.1810(7)	.4352(4)	Al	1/4	1/4	0

*Estimated standard errors refer to the last digit.

†The refined site populations and their proposed ionic species are X(1) = 0.42(1)Ba^{2+} + 0.58(1)□, X(2) = 0.46(1)Ca^{2+} + 0.54(1)□, M(1) = 0.59(1)Fe^{2+} + 0.41(1)Na^{1+}, and M(2) = 0.90(1)Mn^{2+} + 0.10(1) Na^{1+}.

TABLE 3. Samuelsonite. Anisotropic thermal vibration parameters ($\times 10^4$) and equivalent isotropic thermal vibration parameters*

Atom	β_{11}	β_{22}	β_{33}	β_{12}	β_{13}	β_{23}	B(Å^2)
Al	9.3(7)	48.5(43)	12.7(13)	-2.3(15)	6.8(8)	-1.5(19)	0.87
X(1)	28.2(11)	67.1(44)	111.2(32)	0	25.9(15)	0	3.91
X(2)	16.7(15)	72.9(81)	26.5(27)	0	7.1(15)	0	1.71
M(1)	12.4(6)	58.0(33)	14.8(9)	0	6.1(5)	0	1.15
M(2)	10.1(5)	172.8(42)	20.1(9)	0	8.7(5)	0	1.82
Ca(1)	10.56(6)	58.6(29)	18.5(9)	0	7.1(5)	0	1.14
Ca(2)	11.5(6)	52.1(28)	18.5(9)	0	6.5(5)	0	1.16
Ca(3)	17.4(5)	52.4(23)	20.4(7)	1.9(8)	10.6(5)	1.3(9)	1.37
P(1)	9.0(6)	45.7(35)	13.9(11)	0	6.9(6)	0	.87
O(1)	9.4(19)	78.2(114)	20.7(36)	0	6.5(22)	0	1.28
O(2)	14.0(21)	89.7(119)	14.3(33)	0	10.4(22)	0	1.29
O(3)	10.5(13)	48.5(69)	21.2(24)	-6.0(25)	10.2(15)	2.8(34)	1.06
P(2)	9.7(6)	70.4(4)	15.4(11)	0	6.7(7)	0	1.10
O(4)	9.2(19)	55.0(102)	16.5(3)	0	5.5(20)	0	1.04
O(5)	10.4(21)	134.8(140)	15.2(34)	0	6.1(22)	0	1.54
O(6)	17.6(16)	112.3(94)	22.5(26)	-5.3(33)	11.7(17)	-16.6(43)	1.77
P(3)	11.8(7)	49.7(35)	12.5(11)	0	7.4(7)	0	.98
O(7)	12.6(21)	96.4(123)	17.6(34)	0	7.1(23)	0	1.44
O(8)	24.8(27)	73.8(117)	9.8(32)	0	9.9(24)	0	1.58
O(9)	17.5(16)	85.3(85)	14.4(23)	15.2(31)	5.3(16)	-0.8(38)	1.56
P(4)	9.8(7)	55.3(37)	14.0(11)	0	6.4(7)	0	.99
O(10)	12.1(22)	124.8(136)	16.0(35)	0	9.0(23)	0	1.51
O(11)	14.5(22)	74.5(116)	18.5(35)	0	8.1(23)	0	1.39
O(12)	13.2(14)	74.3(80)	23.1(25)	-1.2(29)	8.7(16)	2.4(38)	1.43
P(5)	10.4(7)	43.8(35)	14.5(11)	0	6.6(7)	0	.95
O(13)	20.1(24)	42.5(102)	19.0(34)	0	14.0(24)	0	1.31
O(14)	13.9(23)	106.2(129)	19.7(38)	0	-0.5(24)	0	1.82
O(15)	10.6(13)	56.7(72)	13.9(21)	1.7(26)	5.7(14)	-0.0(33)	1.04
OH	9.0(18)	25.9(91)	19.9(33)	0	9.6(21)	0	.84

*Estimated standard errors refer to the last digit. The β_{ij} terms are coefficients in the expression $\exp-[\beta_{11}h^2 + \beta_{22}k^2 + \beta_{33}\ell^2 + 2\beta_{12}hk + 2\beta_{13}h\ell + 2\beta_{23}k\ell]$.

filled, as inspection of the root mean square displacements and bond distances will demonstrate. The same evidence indicates that Al ($=Al^{3+}$), $(OH)^-$ and the five nonequivalent (PO_4) tetrahedra fully occupy their sites and that no substitutions occur to any significant extent by other ionic species. The positions $X(1)$ and $X(2)$ converged close to half-occupancy at each site, which is required on steric grounds. The $X(1)$–O distances clearly indicate that Ba^{2+} is sequestered at this site. $M(1)$ and $M(2)$ are problematical, since we assumed Na^{1+} substitutes at these sites and that the sites are fully occupied. To achieve full occupancy (indicated by the thermal vibration parameters) we had to ascribe Na^{1+} to these sites. A chemical analysis on a Na-poor samuelsonite from a different location in the pegmatite (see Moore *et al.*, 1975) indicated 8.31 atoms of (Fe^{2+} + Mn^{2+}) in the cell, suggesting that $M(1)$ and $M(2)$ are completely occupied by transition metals for that crystal. Including Na^{1+}, its cell contains 8.51 atoms of (Fe^{2+} + Mn^{2+} + Na^{1+}). The material from which the single crystal was selected for this study afforded 8.04 atoms of (Fe^{2+} + Mn^{2+} + Na^{1+}) (see aforementioned formula). These observations support the proposition that Na^{1+} is distributed over $M(1)$ and $M(2)$ sites. Since the scattering curves for Fe^{2+} and Mn^{2+} are practically indistinguishable, we assumed that Mn^{2+} occupies the larger $M(2)$ site on the basis of a M–O bond distance average of 0.11 Å greater than $M(1)$.

The contents of the formula unit for samuelsonite are presented in Table 1, and it is seen that the results from the structure analysis do not seriously depart from the results of the electron probe analysis. We suggest an "end member" formula

TABLE 4. Samuelsonite. Parameters for the ellipsoids of vibration*

Atom	i	μ_i(x10^2)	θ_{ia}	θ_{ib}	θ_{ic}	Atom	i	μ_i(x10^2)	θ_{ia}	θ_{ib}	θ_{ic}	Atom	i	μ_i(x10^2)	θ_{ia}	θ_{ib}	θ_{ic}
Al	1	12.3	46	110	71	O(2)	1	14.7	38	90	75	P(4)	1	12.3	41	90	72
	2	8.5	134	95	22		2	7.8	128	90	15		2	9.7	131	90	18
	3	10.4	101	159	101		3	14.5	90	180	90		3	11.9	90	180	90
X(1)	1	30.8	98	90	14	O(3)	1	14.3	60	97	53	O(10)	1	17.1	90	0	90
	2	12.5	90	0	90		2	7.2	137	126	53		2	9.3	133	90	20
	3	19.5	172	90	75		3	12.1	62	143	122		3	13.8	137	90	110
X(2)	1	16.0	168	90	56	P(2)	1	12.8	90	0	90	O(11)	1	14.7	29	90	83
	2	13.1	90	0	90		2	10.0	139	90	26		2	11.7	119	90	7
	3	14.9	101	90	146		3	12.4	131	90	116		3	13.2	90	180	90
M(1)	1	13.5	20	90	92	O(4)	1	12.0	62	90	51	O(12)	1	14.6	57	86	55
	2	10.8	110	90	2		2	11.1	152	90	39		2	12.2	134	122	44
	3	11.7	90	180	90		3	11.4	90	180	90		3	13.6	61	147	114
M(2)	1	20.1	90	0	90	O(5)	1	17.8	90	0	90	P(5)	1	12.6	39	90	73
	2	10.0	153	90	41		2	10.6	127	90	14		2	10.0	129	90	17
	3	13.6	116	90	131		3	12.5	143	90	104		3	10.1	90	180	90
Ca(1)	1	13.0	58	90	55	O(6)	1	18.0	68	137	67	O(13)	1	17.5	35	90	78
	2	11.1	148	90	34		2	10.8	118	67	24		2	9.5	125	90	12
	3	11.7	90	180	90		3	15.2	143	124	83		3	10.0	90	180	90
Ca(2)	1	13.1	39	90	74	P(3)	1	13.3	32	90	80	O(14)	1	17.8	153	90	40
	2	11.1	90	0	90		2	8.8	122	90	10		2	11.3	63	90	50
	3	12.0	51	90	164		3	10.8	90	180	90		3	15.8	90	180	90
Ca(3)	1	16.2	33	85	80	O(7)	1	15.0	90	0	90	O(15)	1	12.7	32	70	87
	2	11.0	86	175	90		2	11.6	122	90	9		2	10.3	119	78	14
	3	11.7	58	89	170		3	13.7	148	90	99		3	11.4	102	24	104
P(1)	1	12.1	49	90	63	O(8)	1	19.2	17	90	96	OH	1	13.8	65	90	47
	2	8.7	139	90	27		2	7.6	107	90	6		2	7.8	90	0	90
	3	10.3	90	180	90		3	13.1	90	180	90		3	8.2	24	90	137
O(1)	1	13.5	90	0	90	O(9)	1	18.5	35	55	106						
	2	11.3	173	90	60		2	10.7	110	64	26						
	3	13.2	97	90	150		3	11.7	117	46	109						

* i = i-th principal axis; μ_i = r.m.s. amplitude; θ_{ia}, θ_{ib}, θ_{ic} = angles between i-th principal axis and the cell axes a, b and c.

$(Ca,Ba)Fe_2^{2+}Mn_2^{2+}Ca_8Al_2(OH)_2(PO_4)_{10}$, $Z = 2$, where $X(1)$, $X(2)$ = (Ca,Ba); $M(1) = Fe^{2+}$, $M(2) = Mn^{2+}$, $Ca(1) = Ca(2) = Ca(3) = Ca^{2+}$.

Description of the structure

Owing to a remarkable relationship with the apatite structure type and to important implications in the apatite crystal chemistry, we shall discuss the samuelsonite structure in considerable detail. Samuelsonite is yet another example of an exotic and rare mineral species whose structure admits some inferences and speculations on another more persistent and important structure type.

The samuelsonite crystal structure is very complex (Fig. 1) but with a careful choice of shading and combined use of polyhedral and spoke diagrams, it can be fairly easily visualized. The most pronounced feature is a double column of apatite structure which conserves to a remarkable degree a fragment of the apatite structural topology and geometry. To properly introduce the problem, a few remarks about the apatite structure are appropriate.

Despite the extraordinary persistence of the apatite structure type, from the standpoint of its myriad isotypes and of its bioinorganic as well as inorganic importance, its structure does not easily submit to any simple topological classification. Its closest affinities can be found with the bracelet and pinwheel structures described by Moore (1973). Included here are glaserite, $KNaK_2[SO_4]_2$, $Na_2[SO_4]$ (II), room temperature $K_2[SO_4]$; silicates like merwinite, $Ca_3Mg[SiO_4]_2$, larnite, β-$Ca_2[SiO_4]$, and bredigite, (Ca,Ba) $Ca_{13}Mg_2[SiO_4]_8$; phosphates like $Ba_3[PO_4]_2$, $NaCa[PO_4]$, and brianite, $Na_2CaMg[PO_4]_2$; and the phosphate–silicate silicocarnotite, $Ca_5[PO_4]_2[SiO_4]$ which is a hybrid structure between apatite and glaserite (see Dickens and Brown, 1971, for a detailed description of this structure). Wondratschek (1963), in a study on pyromorphite, has established a formal relationship between the apatite and glaserite structures.

The underlying principle of the apatite structure is a pinwheel comprised of Ca(1) atoms along the trigonal axis at 1/3 2/3 z (and 2/3 1/3 $\bar{z}$), which is sur-

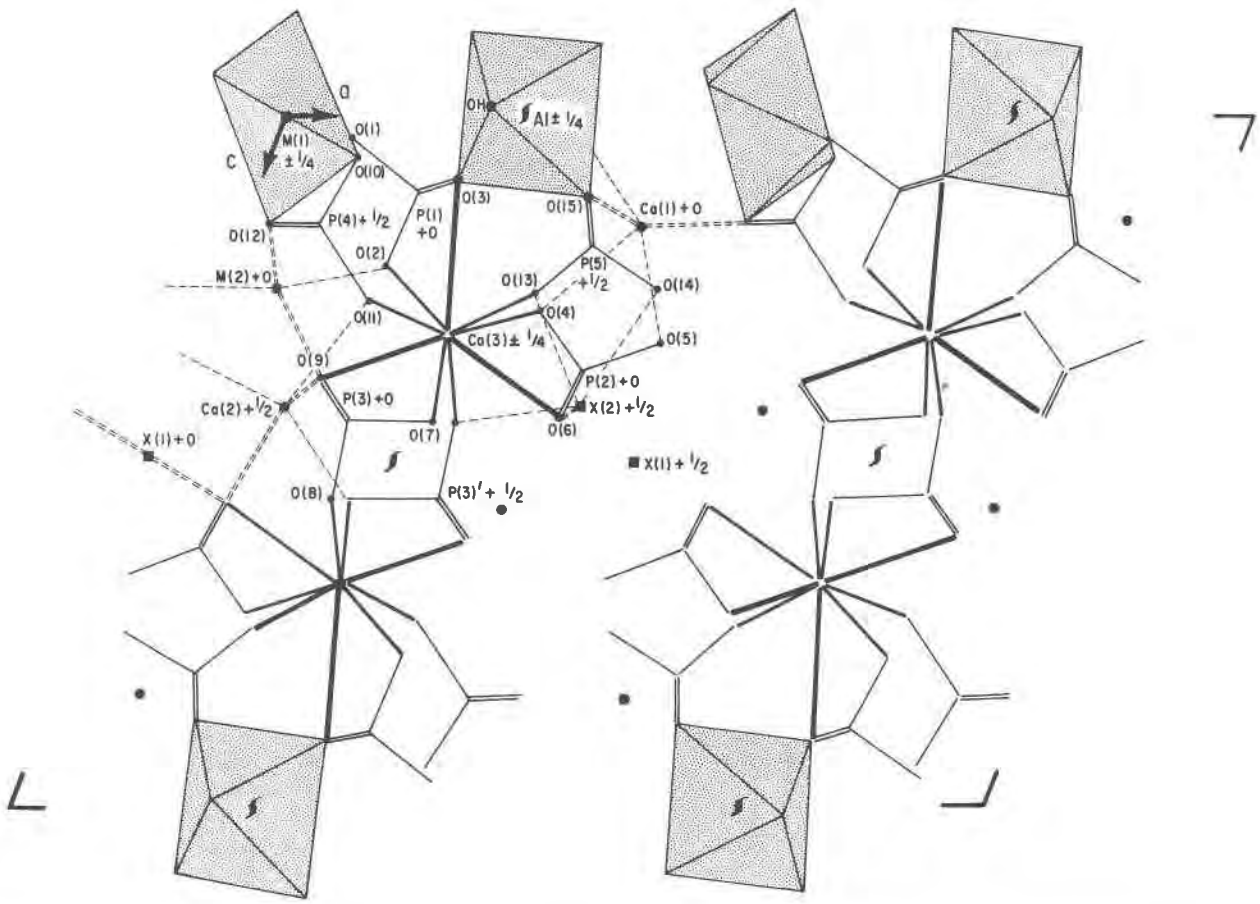

FIG. 1. Diagram of the samuelsonite crystal structure down the *b* axis. The *M*(1)–O and Al–O polyhedra are stippled. *X*(1)–O, *X*(2)–O, *M*(2)–O, Ca(1)–O, and Ca(2)–O bonds are drawn as dashed lines. The P–O bonds are drawn as solid lines, and the Ca(3)–O bonds as solid bold lines. Labeling of the atomic positions conforms with Table 2. Note that some equivalent atoms have been omitted to better express other features of the structure. Some heights are given as fractional coordinates along *b*.

rounded by six linking $[PO_4]$ tetrahedra. The core of the pinwheel is the $Ca(1)O_9$ polyhedron which can be visualized as a distorted cuboctahedron (classified as $F^{[12]}$ in Moore, 1973) with three vacant meridional vertices (Fig. 2b). In many respects, this polyhedron is similar to the more regular $[BaO_9]$ polyhedron in $BaAl_2O_4$ which, like apatite, lacks three meridional occupancies. Continuous rotation of the top and bottom triangular faces leads to the $X^{[12-p]}$, $0 \leq p \leq 6$, polyhedron which is the basis of the pinwheel structure classification of Moore (1973). The value of p determines the number of missing meridional vertices on the polyhedron. Equivalent $Ca(1)O_9$ cores in apatite are fused by face-sharing of the trigonal faces to form a column which runs parallel to the *c* axis. This column, with circumjacent tetrahedra, has formal composition $[Ca_2(PO_4)_6]^{14-}$. The 2_1 screw operations link symmetry equivalent columns together to form the apatite framework, which has the formal cell composition $[Ca_4(PO_4)_6]^{10-}$. The structure is completed by the addition of $[Ca(2)O_6(OH)]$ polyhedra of irregular coordination (described as distorted pentagonal bipyramids) at positions *x y* ¼ *etc.*, resulting in the cell composition $Ca_6(OH)_2[Ca_4(PO_4)_6]$. It is convenient to formulate apatite this way since the $[Ca_2(PO_4)_6]^{14-}$ column is also the key feature of the samuelsonite structure, which is in fact a fragmented apatite.

In samuelsonite, the $[Ca_2(PO_4)_6]^{14-}$ column is fused by a 2_1 operation to an equivalent column to form a double column with formal composition $[Ca_4(PO_4)_{10}]^{22-}$. If extracted from the samuelsonite structure, it can be compared with good coincidence to a double column extracted from apatite (Fig. 3).

Beyond the double column, the structural analogy between samuelsonite and apatite breaks down. This can be seen if the peripheral Ca(2) positions in apatite are superimposed on those of samuelsonite (Fig. 4). In the latter compound, the remaining $X(1)$, $X(2)$, $M(1)$, $M(2)$, Ca(1), Ca(2), and Al positions must be considered. Piecemeal direct comparison of their spoke diagrams in Figure 5 reveals that only Ca(2) in samuelsonite possesses the same kind of environment as Ca(2) in apatite. The $M(1)$ position in samuelsonite is approximately situated along the line (0 0 z) in apatite, but the Al position bears no obvious relationship to an apatite component.

Turning back to Figure 1, it is seen that the $[Ca_4(PO_4)_{10}]^{22-}$ double column is interrupted at $z = 0$ by a barrier of edge-sharing $M(1)O_6$ octahedra and corner-sharing $Al(OH)_2O_4$ octahedra forming $\frac{1}{\infty}[M(1)O_4]$ and $\frac{1}{\infty}[Al(OH)O_4]$ chains which run parallel to the b axis. The remarkable feature of the $\frac{1}{\infty}[Al(OH)O_4]$ chain and its circumjacent linking tetrahedra is that it belongs to the 7 Å octahedral corner-sharing chain structures classified by Moore (1975). Thus, samuelsonite, owing to its $b = 6.80$ Å repeat, is a hybrid structure, sharing qualities of apatite and the 7 Å chain structures (such as childrenite–eosphorite, amblygonite, laueite, *etc.*). In fact, the isomerism of the $\frac{1}{\infty}[Al(OH)O_4]$ chain is of the VI type, *i.e.*, that found in the structure of jahnsite (Moore and Araki, 1974).

At $x = 0$ and $\frac{1}{2}$, another barrier is recognized which further isolates the $[Ca_4(PO_4)_{10}]^{22-}$ double column. Here are located $M(1)$ and $X(1)$; and on either side $M(2)$, $X(2)$, Ca(1), and Ca(2). Although Ca(2) in samuelsonite is isomorphic to Ca(2) in apatite, $X(1)$ and $X(2)$ occur as partly occupied disordered sites, and $M(1)$ and $M(2)$ as distorted octahedra populated by solid solutions of Fe^{2+} and Mn^{2+} with Na^{1+}.

With these facts at hand, it seems plausible to state that the $[Ca_4(PO_4)_{10}]^{22-}$ double column is a stable entity, an argument which will be subsequently employed as a vehicle for a model toward understanding, on structural grounds, the precipitation, nucleation, and growth of apatites; and that the Ca(2) positions in apatites are capable of severe distortions and departures from their ideal loci in the apatite fragmented structures. In other words, the $[Ca_2(PO_4)_6]^{14-}$ column is the template for growth of apatite-like phases and dictates the loci of other cationic species, which evidently are capable of a variety of highly irregular coordinations.

Is it possible to conceptualize a structure which consists of fragmented apatite units such that isolated

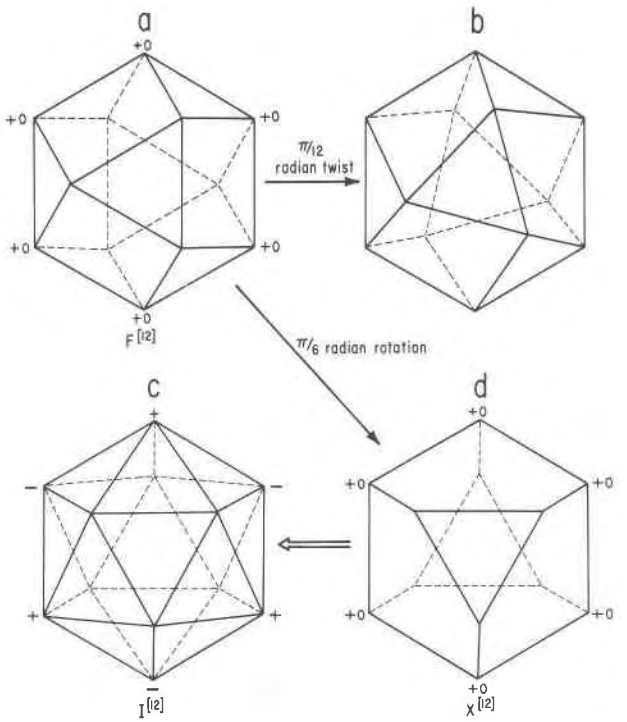

FIG. 2. Relations among the $F^{[12]}$(a), twisted $F^{[12]}$(b), $I^{[12]}$(c), and $X^{[12]}$(d) polyhedra involving movements about an axis normal to the top and bottom triangular faces.

single columns of $[Ca_2(PO_4)_6]^{14-}$ occur? This arrangement can be easily constructed by taking a column in samuelsonite and its linking $\frac{1}{\infty}[Al(OH)O_4]$ chain and orienting the former along the trigonal axis at 1/3 2/3 z and the latter along a 2_1-screw in the $P6_3/m$ cell. The result is an elegant structure in Figure 6. Surrounding the 3-fold axis at 0 0 z is a large cavity of *ca.* 6.5 Å free diameter, and presumably the periphery of this cavity would accommodate the remaining cations of irregular coordination. The cell has dimensions $a \sim 15$, $c \sim 6.8$ Å, space group $P6_3/m$ and contains $X_8^{2+}Al_6(OH)_6[Ca_4(PO_4)_{12}]$ where the X species are the irregular cations. Depending on the charge of X and exploiting the possibilities of partial disorder and irregular coordination, many possibilities are open for accommodating these remaining cations. Incidentally, we have been searching for such a compound in paragenetic settings akin to those observed for samuelsonite. Such crystals would strongly mimic apatite, and on the basis of cell geometry, we would expect them to occur as acicular hexagonal prisms.

It is advantageous to relate the three structures crystal-chemically through expressing their formulae

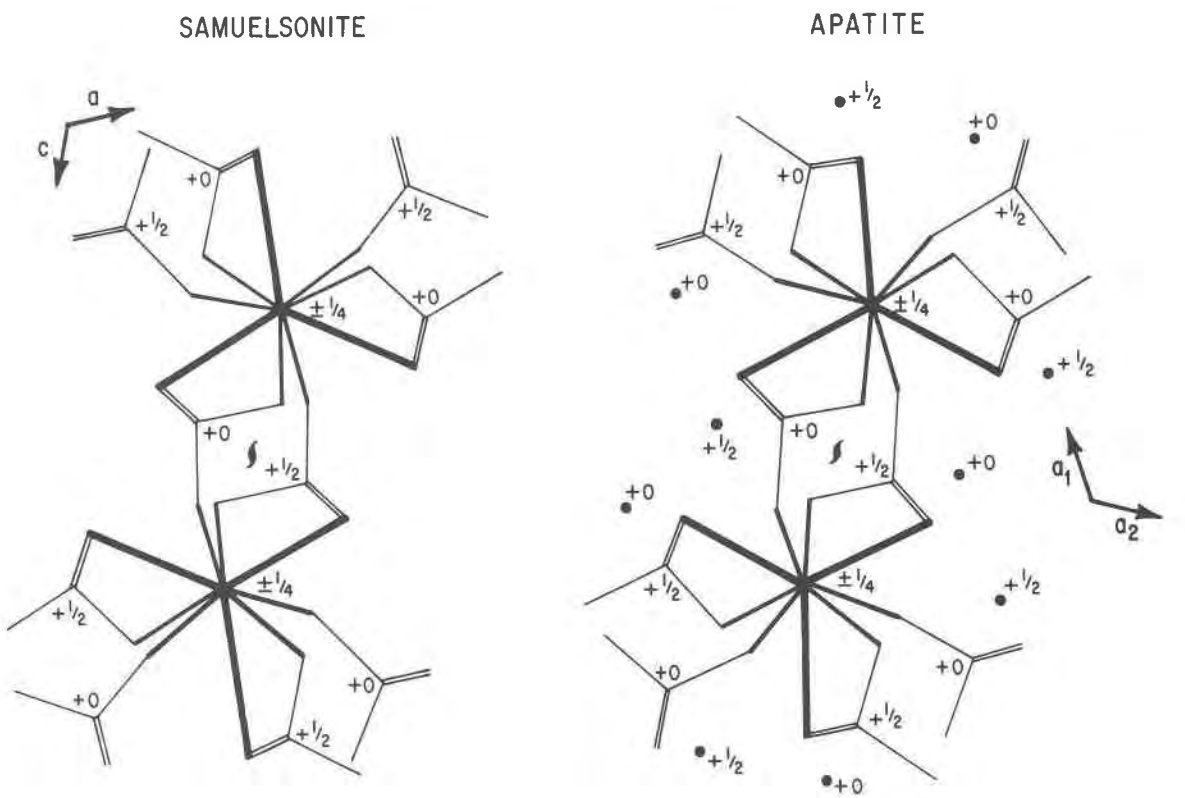

FIG. 3. Isomorphism of the double column in samuelsonite with a fragment of the apatite framework. The origins of the cells refer to samuelsonite (a,c) and apatite (a_1,a_2) respectively. For apatite, the circumjacent Ca(2) loci are indicated as solid disks. Heights are given in fractional coordinates along b in samuelsonite and c in apatite. Note the z coordinate has been shifted $+\frac{1}{4}$ for apatite.

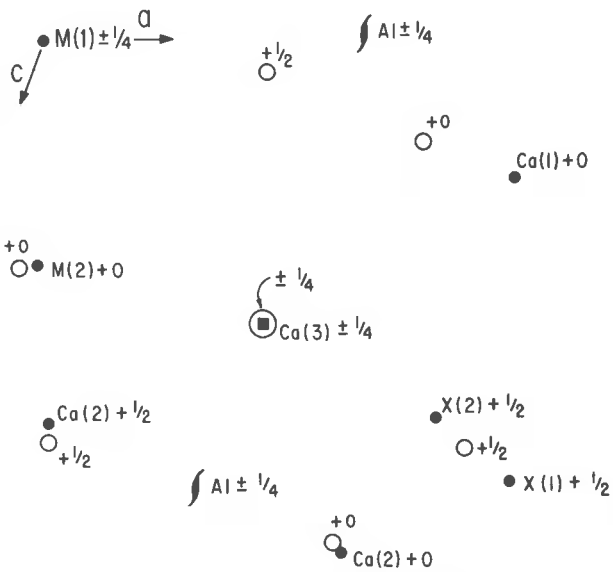

FIG. 4. Comparison of the loci of Al, $X(1)$, $X(2)$, $M(1)$, $M(2)$, Ca(1), and Ca(2) atoms in samuelsonite (solid disks) with Ca(2) in apatite (open circles); and Ca(3) in samuelsonite (solid square) with Ca(1) in apatite (large open circle). The samuelsonite origin is indicated as well as some of its screw axes. Heights are given in fractional coordinates along b in samuelsonite and c in apatite. Note the z coordinate has been shifted $+\frac{1}{4}$ for apatite.

by emphasizing the pinwheel columns in brackets. These formulae would be:

Apatite	$Ca_6(OH)_2$	framework
	$[Ca_4(PO_4)_6]$	columns
Samuelsonite	$(Ba,\square)(Ca,\square)_2$	
	$(Fe,Mn,Na)_4$	double
	$Ca_4Al_2(OH)_2$	column
	$[Ca_4(PO_4)_{10}]$	
Hypothetical	X_8^{2+} $Al_6(OH)_6$	single
	$[Ca_4(PO_4)_{12}]$	column

To test for the stability of such a hypothetical structure, either through attempted synthesis or through search for a natural crystal, is a project of utmost interest, for the existence of such a compound will add further support to the template model of apatite growth proposed further on.

Bond distances and angles

The $M(2)$–, $X(2)$–, Ca(1)–, and Ca(2)–O distances are compared with those for the Ca(2) $(OH)O_6$ polyhedra in apatite in Figure 5. The apatite distances were calculated from the parameters of Sundarsanan and Young (1969) obtained on a Holly Springs hy-

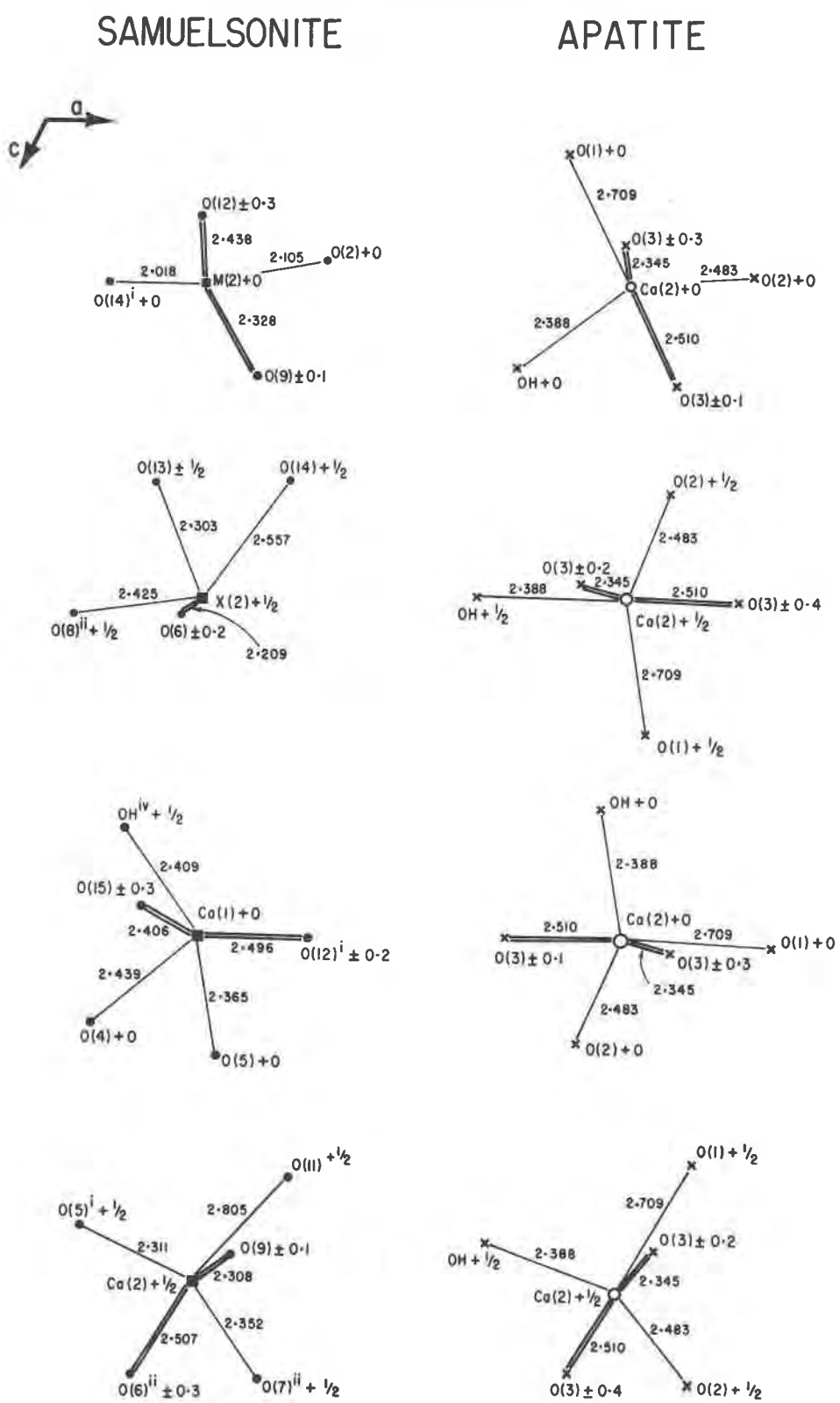

FIG 5. Bond distances for $M(2)$–O, $X(2)$–O, Ca(1)–O and Ca(2)–O for samuelsonite compared with Ca(2)–O for apatite. The apatite Ca(2)–O orientations were made to conform with the cell orientation (a, c) of samuelsonite. Heights are given the same meaning as Fig. 4.

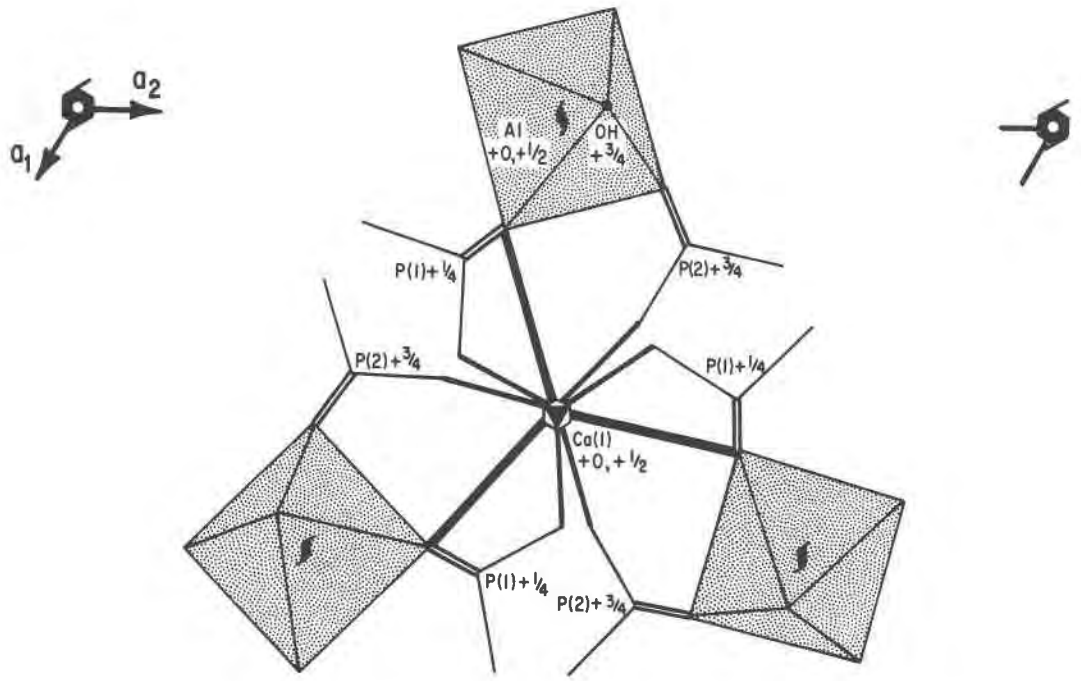

FIG. 6. The hypothetical $X_8^{2+}Al_6(OH)_6[Ca_4(PO_4)_{12}]$ structure, showing the Ca–O bonds, the circumjacent P–O bonds and the Al–O polyhedra. The cell is based on space group $P6_3/m$.

droxylapatite. In this diagram, the $Ca(2)(OH)O_6$ bonds are oriented in such a way that the positions are compatible with Figure 4. The remaining distances are listed in Table 6, as are the O–Me–O′ angles for the $Al(OH)_2O_4$, $M(1)O_6$, $M(2)O_6$, and PO_4 polyhedra. Differences between Ca(3) in samuelsonite and Ca(1) in apatite range up to 0.10 Å for the Ca–O distances and up to 0.30 Å for O–O′ edge distances (see Fig. 7). A range of 0.13 Å difference in Ca(2)–O distances is noted between the $Ca(2)O_7$ polyhedra in both structures.

Coordination numbers proposed in this study include $Al^{[6]}$, $X(1)^{[4]}$, $X(2)^{[5]}$, $M(1)^{[6]}$, $M(2)^{[6]}$, $Ca(1)^{[7]}$, $Ca(2)^{[6+1]}$, $Ca(3)^{[6+3]}$. The coordination numbers for $X(1)$ and $X(2)$ are low for such large cations and probably reflect their disordered nature. Distance averages are Al–O 1.88 Å, $M(1)$–O 2.17 Å, $M(2)$–O 2.28 Å, $X(1)$–O 2.68 Å, $X(2)$–O 2.34 Å, Ca(1)–O 2.43 Å, Ca(2)–O 2.44 Å, Ca(3)–O 2.41 Å (6 inner bonds) and 2.79 Å (3 outer bonds). The P–O averages range from 1.52 to 1.54 Å. The distances are compatible with averages for these cations of similar coordination numbers found in other crystals. In hydroxylapatite, the Ca(1)–O distances are 2.43 Å (6 inner bonds) and 2.80 Å (3 outer bonds), which compare favorably with Ca(3)–O in samuelsonite. The Ca(2)–O 2.47 Å average distance in hydroxylapatite is similar to those for Ca(1) and Ca(2) in samuelsonite. Shannon and Prewitt (1969) suggest Ca–O 2.47 Å for seven-coordinate Ca^{2+}.

One hydrogen bond is proposed for the samuelsonite structure, OH · · · O(10), with a distance of 2.70 Å. Considerations of coordination number and the hydrogen bond permit the assessment of electrostatic valence bond sums of cations about anions (Table 7). In this study we adopt the notation of Baur (1970). For the calculations, $X(1)$, $X(2)$, $M(1)$, and $M(2)$ were treated as divalent species, and the coordination numbers ascribed are those suggested earlier. Bond strengths for the outer bonds of Ca(2) and Ca(3) are distinguished parenthetically. According to this model, the maximum deviations from saturation (p_x = 2.00) are ±0.22 e.s.u. Deviations in bond distances from the polyhedral averages tend to conform with deviations in neutrality except for O(6) and OH. It is possible that some OH^- is replaced by F^-, but owing to the small quantity of material, we cannot test this. It is noted, however, that irregular coordination polyhedra in samuelsonite do not admit certain ascription of coordination numbers, so the valence bond sums are only approximate.

Formation of apatite: an hypothesis

Owing to the important role of apatite and apatite-related phases in bioinorganic chemistry, considerable effort has been directed toward elucidating

TABLE 6. Samuelsonite. Polyhedral interatomic distances and angles*

Al				**X(1)**			
2 Al -OH	1.863			4 X(1)-O(6)	2.684		
2 -O(3)	1.867			2 -X(2)	1.529		
2 -O(15)	1.926						
average	1.885			**Hydrogen Bond**			
				OH···O(10)	2.698		
		O–Al–O′(°)		**P(1)**			
2 OH -O(3)	2.561	86.7		2 P(1)-O(3)	1.519		
2 OH -O(15)^{iv}	2.603	86.8		1 -O(2)	1.546		
2 O(3) -O(15)	2.677	89.8		1 -O(1)	1.552		
2 O(3) -O(15)^{iv}	2.688	90.2		average	1.534		
2 OH -O(3)^{iv}	2.712	93.2					
2 OH -O(15)	2.754	93.2				O–P(1)–O′	
average	2.666	90.0		2 O(2)-O(3)	2.459	106.7	
M(1)				1 O(1)-O(2)	2.495	107.3	
				1 O(3)-O(3)^{iii}	2.502	110.9	
2 M(1) -O(1)	2.067			2 O(1)-O(3)	2.551	112.4	
2 -O(12)	2.157			average	2.503	109.4	
2 -O(10)	2.286						
average	2.170			**P(2)**			
		O–M(1)–O′		1 P(2)-O(5)	1.511		
				1 -O(4)	1.533		
2 O(10)-O(12)	2.466	67.4		2 -O(6)	1.539		
1 O(1) -O(1)^{v}	2.577	77.1		average	1.531		
1 O(10)-O(10)^{v}	2.856	77.3					
2 O(10)-O(12)^{v}	3.131	89.6				O–P(2)–O′	
2 O(1) -O(12)	3.167	97.1		1 O(4)-O(5)	2.440	106.6	
2 O(1)^{v}-O(12)	3.365	105.7		1 O(6)-O(6)^{iii}	2.463	106.3	
2 O(1) -O(10)	3.416	103.3		2 O(4)-O(6)	2.480	107.6	
average	3.043	90.0		2 O(5)-O(6)	2.561	114.2	
M(2)				average	2.498	109.4	
1 M(2) -O(14)^{i}	2.018			**P(3)**			
1 -O(2)	2.105			1 P(3)-O(8)	1.502		
2 -O(9)	2.328			2 -O(9)	1.529		
2 -O(12)	2.438			1 -O(7)	1.531		
average	2.276			average	1.523		
		O–M(2)–O′				O–P(3)–O′	
1 O(9) -O(9)^{iii}	2.454	63.6		1 O(9)-O(9)^{iii}	2.453	106.7	
2 O(2) -O(9)	2.909	81.9		2 O(7)-O(9)	2.466	107.4	
2 O(12)-O(14)^{i}	3.111	88.1		1 O(7)-O(8)	2.474	109.3	
2 O(2) -O(12)	3.169	88.1		2 O(8)-O(9)	2.527	112.9	
2 O(9) -O(12)	3.230	85.2		average	2.486	109.4	
2 O(9) -O(14)^{i}	3.456	105.0					
1 O(12)-O(12)^{iii}	4.317	124.6					
average	3.210	90.4					

P(4)			
1 P(4)-O(11)	1.504		
1 -O(10)	1.536		
2 -O(12)	1.548		
average	1.534		
		O–P(4)–O′	
2 O(10)-O(12)	2.466	106.2	
1 O(12)-O(12)^{iii}	2.487	106.9	
2 O(11)-O(12)	2.518	111.1	
1 O(10)-O(11)	2.563	114.9	
average	2.503	109.4	
P(5)			
1 P(5)-O(13)	1.519		
1 -O(14)	1.536		
2 -O(15)	1.551		
average	1.539		
		O–P(5)–O′	
1 O(13)-O(14)	2.474	108.2	
2 O(13)-O(15)	2.517	110.1	
1 O(15)-O(15)^{iii}	2.521	108.7	
2 O(14)-O(15)	2.527	109.9	
average	2.514	109.5	
Ca(3)			(Apatite)
Ca(3) -O(13)	2.313	(2.405)	
-O(8)^{ii}	2.414	(2.405)	
-O(7)	2.423	(2.456)	
-O(2)	2.435	(2.456)	
-O(4)	2.436	(2.456)	
-O(11)	2.444	(2.405)	
average (inner)	2.411	(2.430)	
-O(6)	2.711	(2.802)	
-O(3)	2.771	(")	
-O(9)	2.899	(")	
average (outer)	2.794	(2.802)	
average (inner + outer)	2.539	(2.554)	

*For other distances, refer to Figs. 5 and 8. Estimated standard errors are within ±0.008Å for P–O, Ca–O and M–O distances; ±0.009A for X(2)–O; and ±0.010 for O–O′.

i = ½+x, ½-y, +z; ii = ½-x, ½+y, -z; iii = x, -y, z; iv = ½-x, ½-y, -z; v = -x, y, -z applied to the coordinates in Table 2.

the chemistry of teeth and bones in the light of stabilities and structural relationships among these phases. In two noteworthy papers on octacalcium phosphate (OCP) and hydroxylapatite (HA), Brown (1962) and Brown *et al.* (1962) have drawn attention to the structure of OCP, $Ca_8H_2(PO_4)_6 \cdot 5H_2O$. This structure, as shown by Brown, possesses 43 nonequivalent atoms in general positions for a triclinic cell

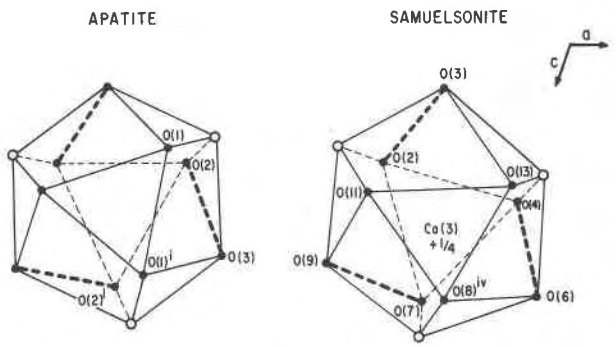

FIG. 7. The Ca(1)–O and Ca(3)–O polyhedra in apatite and samuelsonite respectively referred to the samuelsonite cell orientation (a, c). Empty vertices are shown as open circles, and the bold lines connote edge-sharing with PO_4 tetrahedra.

with parameters a 19.87, b 9.63, c 6.87 Å, α 89°17′, β 92°13′, γ 108°57′, $P\bar{1}$, $Z = 2$. Brown recognized the isomorphism between the region $-\frac{1}{4} < x < \frac{1}{4}$ for this phase with a slab oriented with respect to the $(y\bar{z})$ plane in the apatite structure. Proceeding with an apatite $[Ca_2(PO_4)_6]^{14-}$ column, inversion operations generate a linkage of equivalent columns to form a sheet of composition $^2_\infty[Ca_4(PO_4)_8]^{16-}$ parallel to {100} in OCP. In Figure 8, we have sketched this section of the OCP structure to show its relationship with samuelsonite and HA. Between the sheets, the structure bears no immediate relationship to apatite, although four of the six Ca(2) atoms in apatite (related by the 6_3-operation) are tucked into similar positions in OCP. The obvious structural similarity of OCP to apatite and samuelsonite prompts us to write its formula as $Ca_{12}(PO_3OH)_4 \cdot 10H_2O \cdot [Ca_4(PO_4)_8]$, the region in brackets expressing the apatite columns. The observation that Ca:P ratios in precipitated calcium phosphates which yield apatite X-ray patterns are often less than that of HA; the platy development of octacalcium phosphate crystals and the observation that platy to acicular habits for apatitic crystallites occur in bone; the epitaxial relation between the (a_2, b) and (c, c) axes of (HA, OCP); and the hydrolysis of OCP to form crystalline HA led Brown *et al.* (1962) to suggest that OCP may be an important intermediary in bioinorganic production of bone and tooth material.

From the results of radial distribution analysis of amorphous calcium phosphate (ACP) precipitates, Betts and Posner (1974a, b) have proposed a cluster model which is a spheroidal fragment of the HA unit cell and which possesses composition $Ca_9(PO_4)_6$. The model involves three of the columnar Ca(1) cations, the six circumjacent Ca(2) cations, and the six associated (PO_4) tetrahedra. Based on an assumed 9.5 Å diameter for the cluster, a reduced intensity function, $F(s)$, was calculated from the atomic coordinates of the HA structure. The observed and calculated $F(s)$ curves were shown to be in good agreement, providing the calculated cluster is dilated by about 3 percent. From the model, Betts and Posner (1974) proceeded to calculate cluster densities for ACP.

If such a cluster is intrinsically stable and represents an equilibrium configuration in solution as well as in crystals, then every effort should be expended to test its existence in other crystal structures, especially in crystalline solvates. It seems appropriate, therefore, to inquire further about the geometrical quality of the cluster. Since double columns, sheets, and frameworks built of the same module are now characterized, it is appealing to commence with a cluster model based on the unit isomorphic to the three structure types: the $[Ca(PO_4)_6]^{16-}$ cluster. This cluster incorporates the Ca(1) position and the circumjacent tetrahedra in HA. Note that the circumjacent Ca(2) in the HA structure type do *not* possess isomorphisms in the OCP and samuelsonite structures. Owing to the remarkable coincidence of the $[Ca_2(PO_4)_6]^{14-}$ columns in all three structures, we conclude that the stability of the apatite structure type is dominated by the columns of which the $[Ca(PO_4)_6]^{16-}$ cluster is the module.

An interesting cluster of similar type is found in the crystal structure of hanksite, $KNa_{22}(CO_3)_2(SO_4)_9Cl$, the structure of which was reported by Araki and Zoltai (1973). In this structure, a central $[K(SO_4)_6]^{11-}$ cluster can be discerned. The central K^{1+} cation is surrounded by six oxygens, at K–O(6) = 2.93 Å, which define a trigonal antiprism, and by six additional meridional oxygens at K–O(8) = 3.13 Å. A sketch (Fig. 9) of the central KO_{12} polyhedron and the six circumjacent $[S(2)O_4]$ tetrahedra shows that it is a distorted cuboctahedron. The point groups of the distorted cuboctahedral clusters in hanksite and HA are $\bar{3}$ and 3 respectively. Comparisons of hanksite with the $Ca(1)O_{9\square 3}$ polyhedron and the six $[PO_4]$ tetrahedra in HA (Fig. 9) reveals that alternate tetrahedra are arranged similarly in both structures, that is a set which obeys 3-fold rotational symmetry. The remaining three tetrahedra each donate two oxygens to the hanksite polyhedron but only one to HA. Since continuous relationships among the cuboctahedron, $X^{[12]}$ and the icosahedron have been demonstrated, it is clear that these clusters are approximations to local densest packings. We add that a column can be iden-

TABLE 7. Samuelsonite. Electrostatic bond strength–bond length relationships*

	Al	X(1)	X(2)	M(1)	M(2)	Ca(1)	Ca(2)	Ca(3)	P(1)	P(2)	P(3)	P(4)	P(5)	Hd	Ha	Δpx
O(1)	--	----	----	2	----	-----	-----	-----	1	----	----	----	----	--	--	-0.08
O(2)	--	----	----	----	1	-----	-----	2	1	----	----	----	----	--	--	+0.02
O(3)	1	----	----	----	----	-----	-----	(1)	1	----	----	----	----	--	--	-0.03
O(4)	--	----	----	----	----	1	-----	2	----	1	----	----	----	--	--	(-0.25) -0.02
O(5)	--	----	----	----	----	1	1	-----	----	1	----	----	----	--	--	-0.17
O(6)	--	½	½	----	----	-----	1	(1)	----	1	----	----	----	--	--	+0.21
O(7)	--	----	----	----	----	-----	1	2	----	----	1	----	----	--	--	(-0.01) -0.02
O(8)	--	----	½	----	----	-----	-----	2	----	----	1	----	----	--	--	-0.11
O(9)	--	----	----	----	1	-----	1	(1)	----	----	1	----	----	--	--	+0.09
O(10)	--	----	----	2	----	-----	-----	-----	----	----	----	1	----	--	1	(-0.13) +0.09
O(11)	--	----	----	----	----	-----	1	2	----	----	----	1	----	--	--	-0.02
O(12)	--	----	----	1	1	1	-----	-----	----	----	----	1	----	--	--	+0.21
O(13)	--	----	½	----	----	-----	-----	2	----	----	----	----	1	--	--	-0.11
O(14)	--	----	½	----	1	-----	-----	-----	----	----	----	----	1	--	--	-0.22
O(15)	1	----	----	----	----	1	-----	-----	----	----	----	----	1	--	--	+0.04
OH	2	----	----	----	----	1	-----	-----	----	----	----	----	----	1	--	+0.12

Δd

	Al	X(1)	X(2)	M(1)	M(2)	Ca(1)	Ca(2)	Ca(3)	P(1)	P(2)	P(3)	P(4)	P(5)
O(1)	--	----	----	-0.10 -0.10	----	-----	-----	-----	+0.02	----	----	----	----
O(2)	--	----	----	----	-0.17	-----	-----	+0.02	+0.01	----	----	----	----
O(3)	-0.02	----	----	----	----	-----	-----	+0.02 (+0.23)	-0.02	----	----	----	----
O(4)	--	----	----	----	----	+0.01	-----	+0.02	----	+0.00	----	----	----
O(5)	--	----	----	----	----	-0.07	-0.13	+0.02 -----	----	-0.02	----	----	----
O(6)	--	+0.00	-0.13	----	----	-----	+0.06	(+0.27)	----	+0.01	----	----	----
O(7)	--	----	----	----	----	-----	-0.09	+0.01, +0.01	----	----	+0.01	----	----
O(8)	--	----	+0.08	----	----	-----	-----	+0.00, +0.00	----	----	-0.02	----	----
O(9)	--	----	----	----	+0.05	-----	-0.13	(+0.36)	----	----	+0.01	----	----
O(10)	--	----	----	+0.12, +0.12	----	----	-----	-----	----	----	----	+0.00	----
O(11)	--	----	----	----	----	-----	+0.36	+0.03, +0.03	----	----	----	-0.03	----
O(12)	--	----	----	-0.01	+0.16	+0.06	-----	-----	----	----	----	+0.01	----
O(13)	--	----	-0.04	----	----	------	-----	-0.11	----	----	----	----	-0.02
O(14)	--	----	+0.22	----	-0.16	-----	-----	-0.11 ----	----	----	----	----	+0.00
O(15)	+0.04	----	----	----	----	-0.03	-----	-----	----	----	----	----	+0.01
OH	-0.02	----	----	----	----	-0.02	-----	-----	----	----	----	----	----

*Number of cations bonded to anions are listed. The deviation from electrostatic neutrality, Δpx, is given. Outer shell coordination for Ca(3) is listed parenthetically. Deviations in bond distances, Δd, from polyhedral averages are listed.

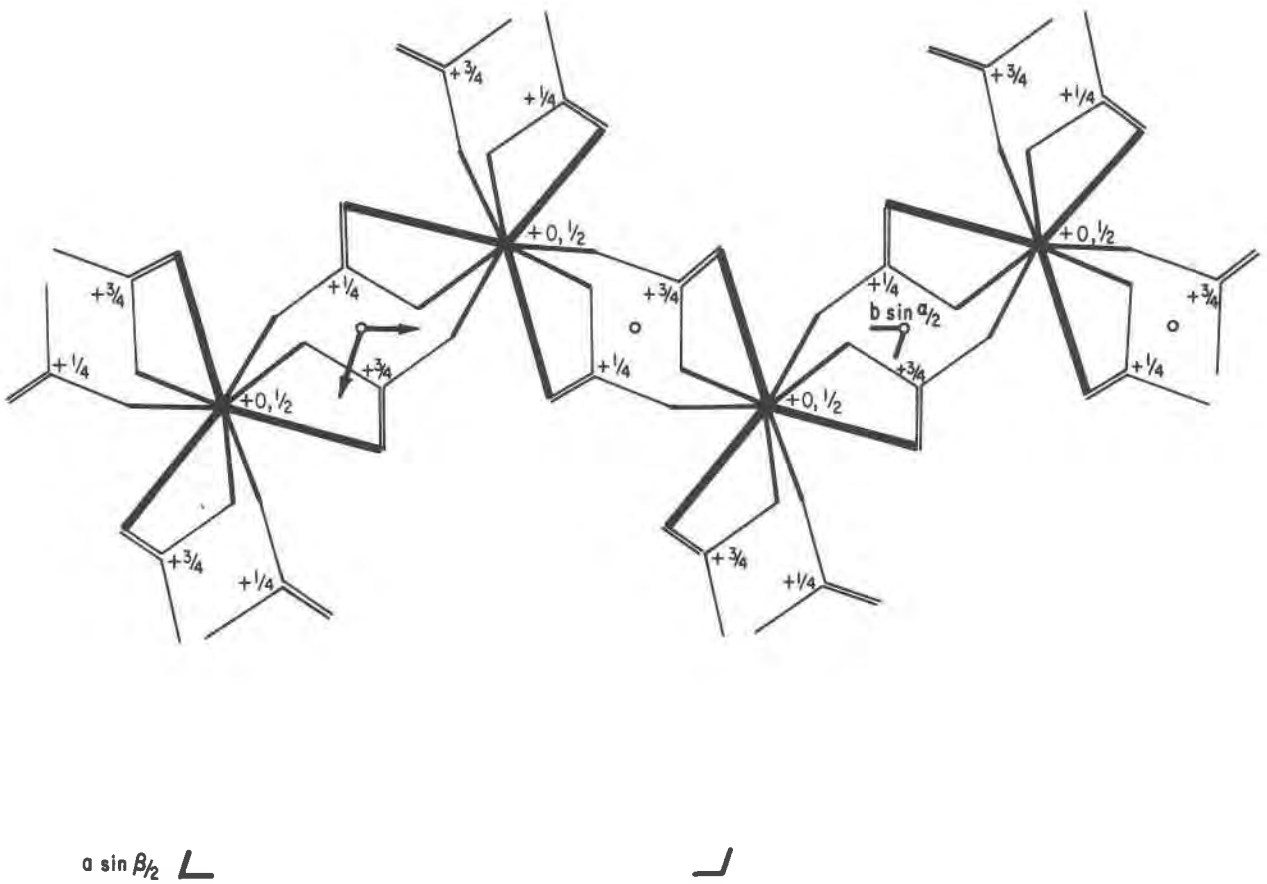

FIG. 8. Portion of the octacalcium phosphate structure featuring the condensed Ca–O columns and circumjacent tetrahedra. The coordinates for this sketch are from Brown (1962). Heights, slightly idealized, are given as fractional coordinates.

tified in the hanksite *c*-axial repeat: it is comprised of an aliquot of two $[K(SO_4)_6]^{11-}$ interleaved by four NaO_6 octahedra, two above and two below; and six additional connecting $[S(1)O_4]$ tetrahedra, that is, $\frac{1}{c}[KNa_2(SO_4)_9]^{15-}$. For this reason, we prefer to express the hanksite formula as $Na_{20}(CO_3)_2Cl[KNa_2(SO_4)_9]$.

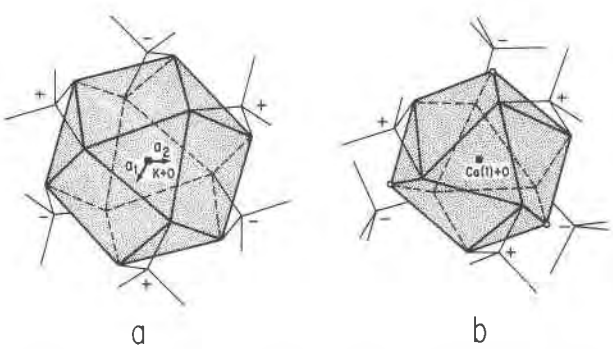

FIG. 9. The K–O polyhedron and the six circumjacent S–O bonds in hanksite (a), and the Ca(1)–O polyhedron and its six circumjacent P–O bonds in hydroxyl-apatite (b). The drawings were constructed directly from the atomic coordinates of Araki and Zoltai (1973) for hanksite, and Sudarsanan and Young (1969) for hydroxylapatite.

With the above information at hand, we offer an hypothesis for apatite formation and the formation of related phases. Despite insufficient evidence, we feel that the hypothesis is testable and that the hypothesis at the very least delineates several interesting problems in the crystal chemistry of solvate complexes. In addition, it aids in selecting those structures which should be further examined in detail with respect to local isomorphisms of their clusters. Included are the crystalline oxysalts of intermediate to large alkali and alkaline earth cations, especially the phosphates, sulfates, vanadates, and silicates.

Hypothesis 1. The modular unit is $[Ca(PO_4)_6]^{16-}$

The cluster has a configuration like that found in hanksite, with two tetrahedral vertices bonded to the central cation. Such a cluster may have formal charge $\{Ca[PO_2(OH)_2]_6\}^{4-}$ in solution. A related cluster can be identified in the crystal structure of $Ca(H_2O)$

$[PO_2(OH)_2]_2$, determined by Jones and Cruickshank (1961). The environment about Ca^{2+} is shown in Figure 10. The polyhedron can be recognized as a twisted cuboctahedron with four missing meridional vertices and resembles the polyhedron found in HA. Five circumjacent tetrahedra can be discerned, and two of these share edges, the remaining three sharing corners. In place of a tetrahedral bond at one antiprismatic face, there is the water molecule. Athough the order of the tetrahedra around the large polyhedron is different than in HA, the bond distances and their distortions of the polyhedron are similar to those found in HA.

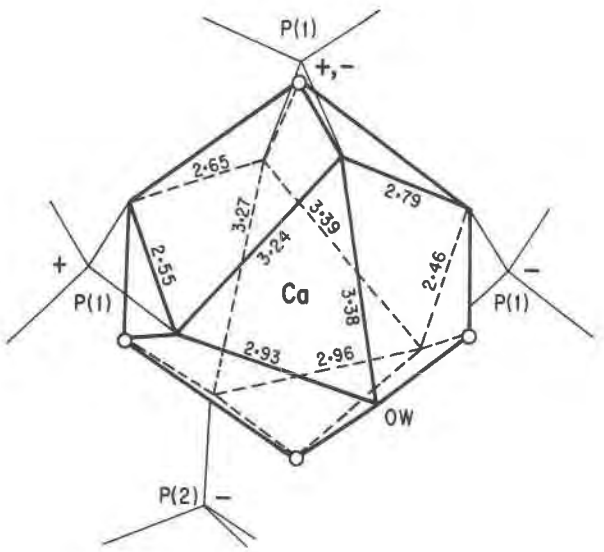

FIG. 10. The polyhedron around Ca and the circumjacent tetrahedra in the crystal structure of $Ca(H_2O)[PO_2(OH)_2]_2$. The coordinates are from Jones and Cruickshank (1961).

Hypothesis 2. The cluster of Betts and Posner proceeds from the modular unit

Adding two Ca^{2+} above and below the trigonal faces in the hanksite arrangement leads to the trimeric cluster $\{[(H_2O)_3Ca]_2Ca(PO_4)_6\}$. In many respects, it resembles the local arrangement found in hanksite, with the two additional Ca^{2+} octahedrally

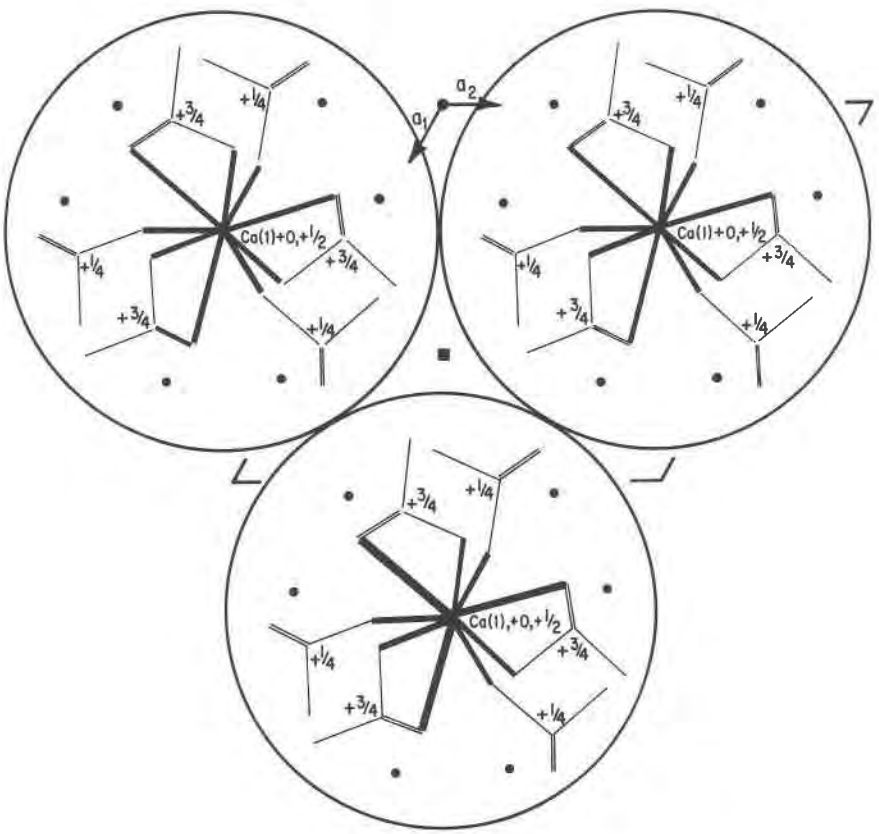

FIG. 11. The hexagonal close-packing of $[Ca_2(PO_4)_6]^{14}$ columns and the associated Ca(2) cations leads to the apatite framework with missing Ca at 2/3 1/3 0 and 2/3 1/3 1/2, and OH^- at 0 0 z. The diameter for the cylinder corresponds to that of Betts and Posner (1974*b*).

coordinated, the terminal trigonal faces consisting of bound water molecules.

Hypothesis 3. Polymerization proceeds through growth of the column and columns pack densely

The ordered $[Ca_2(PO_4)_6]$ column grows more rapidly than the lateral growth between clusters. Such growth would lead to disorder not along the columns but between them in the HA crystal. Figure 11 illustrates how the cylindrical packing of these columns leads to the HA framework structure. Note that the peripheral Ca(2) are included, but that the Ca(1) at $(x,y) = (2/3, 1/3)$ are missing.

From this model, disorder in HA crystals can be conceived as local misfits of the Ca(2) atoms about the central column and as rotational disorder of columns relative to each other. The study of Betts and Posner (1974b) would suggest that the Ca(2) atoms are "carried over" by the symmetry of the central column fragment. It would appear, then, that rotational disorder of the columns is more likely. Morphological characters of natural and synthetic apatites support this assertion. Crystals of apatites, especially those found in low-temperature assemblages, often show a fibrous aspect, consisting of stalks or bundles of individual fibrils. Rotation photographs about the *c* axis from such crystals show layer lines which are sharp but Weissenberg photographs which show continuous streaks.

Concluding remarks

The persistence of $[Ca_2(PO_4)_6]$ columns, in the crystal structures of three distinct phases, samuelsonite, octacalcium phosphate, and apatite, suggest that the column dictates the structural aspect and that growth proceeds through condensation of the columns. Applied to the apatite structure type, this implies that disorder arises from the cylindrical packing of the columns with rotational disorder of these columns leading to stalk-like and fibrous development of crystals. Since the $[Ca_9(PO_4)_6]$ cluster model of Betts and Posner (1974b) suggests that the Ca(2) atoms are carried along with the column's core, and since the column is the only readily identifiable unit isomorphic to three distinct structure types, the hypothesis that disorder arises from column misfits is appealing.

Calcium-deficient apatites need not require the presence of another phase such as OCP to explain these stoichiometric deviations; rotational disorder of packed columns can achieve the same result. In such a model, the calcium deficit appears in the Ca(1) positions which remain after columns are densely packed. Annealing of disordered crystals, for such a model, can be achieved by rotations of extensive subunits of the structure—in this case the columns—with the addition of Ca(1) at the stabilized site to provide additional bonds necessary for local electrostatic neutrality of terminal phosphate oxygens.

Acknowledgments

This study was supported by the N.S.F. Ga-40543 (Geochemistry Section) grant awarded to P. B. M. and a Materials Research Laboratory (N.S.F.) grant awarded to The University of Chicago.

References

Araki, T. and T. Zoltai (1973) The crystal structure of hanksite. *Am. Mineral., 58,* 799–801.

Baur, W. H. (1970) Bond length variation and distorted coordination polyhedra in inorganic crystals. *Trans. Am. Crystallogr. Assoc. 6,* 129–155.

Betts, F. and A. S. Posner (1974a) An X-ray radial distribution study of amorphous calcium phosphate. *Mater. Res. Bull. 9,* 353–360.

——— (1974b) A structural model for amorphous calcium phosphate. *Trans. Am. Crystallogr. Assoc., 10,* 73–84.

Brown, W. E. (1962) Octacalcium phosphate and hydroxyapatite. *Nature, 196,* 1048–1050.

———, J. P. Smith, J. R. Lehr and A. W. Frazier (1962) Crystallographic and chemical relations between octacalcium phosphate and hydroxyapatite. *Nature, 196,* 1050–1055.

Burnham, C. W. (1966) Computation of absorption corrections, and the significance of the end effect. *Am. Mineral, 51,* 159–167.

Cromer, D. T. and J. B. Mann (1968) X-ray scattering factors computed from numerical Hartree-Fock wave-functions. *Acta Crystallogr, A24,* 321–324.

Dickens, B., and W. E. Brown (1971) The crystal structure of $Ca_5(PO_4)_2(SiO_4)$(silico-carnotite). *Tschermaks Mineral. Petrogr. Mitt., 16,* 1–27.

Finger, L. W. (1968) Determination of cation distribution by least-squares refinement of single crystal x-ray data. *Carnegie Inst. Wash. Year Book, 67,* 216–217.

Howells, E. R., D. C. Phillips and D. Rogers (1950) The probability distribution of X-ray intensity. II. Experimental investigation on the X-ray detection of center of symmetry. *Act. Crystallogr., 3,* 210–214.

Jones, D. W. and D. W. J. Cruickshank (1961) The crystal structures of two calcium orthophosphates: $CaHPO_4$ and $Ca(H_2PO_4)_2 \cdot H_2O$. *Z. Kristallogr., 116,* 101–125.

Moore, P. B. (1973) Bracelets and pinwheels: A topological–geometrical approach to the calcium orthosilicate and alkali sulfate structures. *Am. Mineral. 58,* 32–42.

——— (1975) Laueite, pseudolaueite, stewartite and metavauxite: a study in combinatorial polymorphism. *Neues Jahrb. Mineral. Abh., 123,* 148–159.

——— and T. Araki (1974) Jahnsite, $CaMn^{2+}Mg_2(H_2O)_8Fe^{3+}_2(OH)_2[PO_4]_4$: a novel stereoisomerism of ligands about octahedral corner-sharing chains. *Am. Mineral., 59,* 964–973.

———, A. J. Irving and A. R. Kampf (1975) Foggite, $CaAl(OH)_2(H_2O)[PO_4]$; goedkenite, $(Sr,Ca)_2l(OH)[PO_4]_2$; and

samuelsonite, $(Ca,Ba)Fe_2^{2+}Mn_2^{2+}Ca_8Al_2(OH)_2[PO_4]_{10}$: three new species from the Palermo No. 1 pegmatite, North Groton, New Hampshire. *Am. Mineral., 60,* 957–964.

Ramachandran, G. N. and R. Srinivasan (1970) *Fourier Methods in Crystallography.* Wiley-Interscience, New York, 96–119.

Shannon, R. D. and C. T. Prewitt (1969) Effective ionic radii in oxides and fluorides. *Acta Crystallogr., B25,* 925–946.

Srikrishnan, T. and S. Parthasarathy (1970) A modified $N(y)$ test for centrosymmetry for crystals containing heavy atoms. *Z. Kristallogr., 131,* 186–195.

Sudarsanan, K. and R. A. Young (1969) Significant precision in crystal structure details: Holly Springs hydroxyapatite. *Acta Crystallogr., B25,* 1534–1543.

Wondratscheck, H. (1963) Untersuchungen zur Kristallchemie der Blei-Apatite (Pyromorphite). *Neues Jahrb. Mineral. Abh., 99,* 113–160.

Zachariasen, W. H. (1968) Experimental tests of the general formula for the integrated intensity of a real crystal. *Acta Crystallogr., A24,* 212–214.

Manuscript received, February 17, 1976; accepted for publication, September 13, 1976.